Increased Choroidal Vascularity in Central Serous Chorioretinopathy Quantified Using Swept-Source Optical Coherence Tomography

YOSHIMASA KURODA, SOTARO OOTO, KENJI YAMASHIRO, AKIO OISHI, HIDEO NAKANISHI, HIROSHI TAMURA, NAOKO UEDA-ARAKAWA, AND NAGAHISA YOSHIMURA

• PURPOSE: To investigate the choroidal vascular structural changes in eyes with central serous chorioretinopathy (CSC) by using swept-source optical coherence tomography (SS-OCT).

• DESIGN: Prospective cross-sectional study.

• METHODS: We prospectively examined 40 eyes of 34 consecutive patients with CSC. Three-dimensional choroidal images of the macular area, covering 3 × 3 mm and 6 × 6 mm, were obtained with SS-OCT. En face images of the microvasculature of the inner choroid and large choroidal vessel layers were converted to binary images. Choroidal vascular areas were analyzed quantitatively using the binary images.

• RESULTS: The choroidal vascular area was larger in eyes with CSC (the microvasculature of the inner choroid: 53.4% ± 2.4%, $P = .028$; 3 × 3-mm large choroidal vessels: 66.9% ± 7.1%, $P < .001$; and 6 × 6-mm large choroidal vessels: 64.8% ± 7.3%, $P < .001$) than in age-matched normal eyes (52.2% ± 1.8%, 54.9% ± 4.4%, and 53.8% ± 4.3%, respectively). The choroidal vascular area at the microvasculature of the inner choroid level was larger in multifocal posterior pigment epitheliopathy (55.8% ± 2.2%) than in classic CSC (53.1% ± 2.1%, $P = .038$) and in diffuse retinal pigment epitheliopathy (52.9% ± 2.6%, $P = .042$). The subfoveal choroidal thickness was significantly associated with the choroidal vascular area at the level of large choroidal vessels ($P < .001$).

• CONCLUSIONS: Increased choroidal vascular area was observed in the whole macula area in eyes with CSC. This finding suggests that CSC may originate from a choroidal circulatory disturbance. (Am J Ophthalmol 2016;169:199–207. © 2016 Elsevier Inc. All rights reserved.)

AJO.com Supplemental Material available at AJO.com.

Accepted for publication Jun 29, 2016.

From the Department of Ophthalmology and Visual Sciences, Kyoto University Graduate School of Medicine, Kyoto, Japan.

Inquiries to Sotaro Ooto, Department of Ophthalmology and Visual Sciences, Kyoto University Graduate School of Medicine, 54 Kawahara, Shogoin, Sakyo, Kyoto 606-8507, Japan; e-mail: ohoto@kuhp.kyoto-u.ac.jp

CENTRAL SEROUS CHORIORETINOPATHY (CSC) IS characterized by serous retinal detachment (SRD) in the macula accompanied with retinal pigment epithelium (RPE) detachment.[1–5] Fluorescein angiography (FA) shows a single or multiple points of dye leakage at the RPE and dye pooling into the subretinal space.[6] The subretinal fluid may be derived from the choroidal exudation.[7] In addition, indocyanine green angiography (IA) shows choroidal vascular changes, including delayed filling, vascular congestion, choroidal hyperpermeability, and punctate hyperfluorescent spots.[8–14] These angiographic findings strongly suggest that the primary mechanism underlying CSC may involve a choroidal vascular abnormality.

Imaging of the choroid with optical coherence tomography (OCT) does not allow visualization of the entire choroidal structure, owing to its low penetration and high backscattering at the level of the RPE. However, since Margolis and Spaide introduced enhanced depth imaging (EDI) OCT,[15] many investigators have studied choroidal thickness in healthy and diseased eyes. In fact, using the EDI-OCT technique, it has been reported that choroidal thickness increased in patients with CSC compared with that in patients with normal eyes.[16,17] However, EDI-OCT is usually coupled to multiple averaging to achieve high contrast and low speckle noise, resulting in less detailed raster scan images. For this reason, en face imaging of the choroid is difficult using EDI-OCT.

Other investigators reported the measurement of choroidal thickness with the use of OCT at a longer wavelength.[18–20] Swept-source (SS)-OCT at a longer wavelength, which is characterized by a high-speed scan rate and a relatively low-sensitivity roll-off vs depth compared with the spectral-domain OCT, allows us to obtain a 3-dimensional (3D) high-contrast image of the choroid.[21] In addition, several algorithms were recently developed for SS-OCT, which allows for en face imaging of the choroid. These developments provide the unique opportunity to profile the 3D anatomy of choroidal layers.[22–24]

The purpose of this study was to objectively assess the choroidal vascular dilation in eyes with CSC using en face SS-OCT imaging. We scanned the whole macular area of healthy subjects and CSC patients by high-penetrating SS-OCT using a 3D scan protocol, and produced en face images of the microvasculature of the inner

0002-9394/$36.00
http://dx.doi.org/10.1016/j.ajo.2016.06.043

choroid and large choroidal vessels. We converted en face images obtained by SS-OCT into binary images and assessed the enlarged choroidal vasculature quantitatively.

METHODS

THE ETHICS COMMITTEE AT KYOTO UNIVERSITY GRADUATE School of Medicine approved this prospective study, which was conducted in accordance with the tenets of the Declaration of Helsinki. Written informed consent was obtained from each subject before any study procedures or examinations were performed.

• **SUBJECTS:** For this prospective cross-sectional study, we recruited consecutive patients with CSC who visited the Macular Service at Kyoto University Hospital between January 2014 and November 2014, as well as age-matched healthy subjects. Healthy eyes were recruited from healthy volunteers and unaffected fellow eyes of patients with unilateral retinal diseases (eg, epiretinal membrane, vitreomacular traction syndrome). All of the subjects underwent a comprehensive ocular examination, including autorefractometry, best-corrected visual acuity measurement with a Landolt C chart, slit-lamp biomicroscopy, intraocular pressure measurement, fundus photography (TRC-NW8F; Topcon Corp, Tokyo, Japan), axial length measurement using ocular biometry (IOLMaster; Carl Zeiss Meditec, Jena, Germany), and SS-OCT imaging (DRI OCT-1; Topcon Corp). All patients with CSC also underwent simultaneous FA and IA using the Spectralis HRA+OCT (Heidelberg Engineering, Heidelberg, Germany). CSC was diagnosed if patients had SRD within the macular area, which was confirmed by OCT, and associated with idiopathic leaks from the RPE during FA/IA, excluding other causes of SRD. The exclusion criteria included other macular abnormalities (eg, retinal vein occlusion, age-related macular degeneration, pathologic myopia, idiopathic choroidal neovascularization [CNV], other secondary CNV, intraocular inflammation, history of ocular trauma, poor image owing to media opacity or poor fixation, or history of vitrectomy, anti–vascular endothelial growth factor administration, and photodynamic therapy).

• **CLASSIFICATION OF CENTRAL SEROUS CHORIORETINOPATHY:** Patients with CSC were classified into 3 types: classic CSC, diffuse retinal pigment epitheliopathy (DRPE), and multifocal posterior pigment epitheliopathy (MPPE).[25] Classic CSC was defined as only a few spots of leakage from the RPE.[2] DRPE was defined as broad areas of granular hyperfluorescence during FA associated with many indistinct areas of leakage.[2] MPPE was defined as multiple massive leakages from the choroid.[25]

Each type of CSC was divided into active and resolved eyes. Active eye was indicated when the eye had SRD within the macular area. Resolved eye was indicated as the absence of SRD at the time of SS-OCT measurement, showing SRD at the first visit or at the visit before the time of SS-OCT measurement.

• **SWEPT-SOURCE OPTICAL COHERENCE TOMOGRAPHY:** Swept-source OCT examinations were performed by trained examiners after pupil dilation. In each subject, horizontal and vertical line scans (12 mm) were obtained through the fovea. Each 3D volumetric scan covered an area of 3×3 mm^2 and 6×6 mm^2, centered on the fovea. Three-dimensional 3×3-mm^2 volumetric scans consisted of 512 (horizontal) $\times$ 256 (vertical) A-scans and 3D 6×6-mm^2 volumetric scans comprised 512 (horizontal) $\times$ 128 (vertical).

• **MEASUREMENT OF CHOROIDAL THICKNESS:** Choroidal thickness was defined as the distance between the line corresponding to the Bruch membrane beneath the RPE and the chorioscleral interface. The choroidal thicknesses at the center of the fovea were manually measured from vertical and horizontal scans with a built-in caliber tool, and each length was averaged.

• **EN FACE IMAGING:** In each B-scan of the 3D data set, the outer surface of the Bruch membrane line was automatically determined by the software, and manual corrections were made as necessary using the built-in segmentation-modifying tool. En face images were automatically reconstructed from the 3D data set using software developed by Topcon Corporation. En face images of the choroid were created by being extracted at varying depths every 2.6 μm from the Bruch membrane and were flattened at the level of the Bruch membrane. In the middle row of Figure 1, the en face images indicated white region for vascular lumens and black region for the vascular wall and choridal stroma.

• **MEASUREMENT OF CHOROIDAL VASCULAR AREA:** To evaluate the area of choroidal vasculature, 2 en face images were used: 1 at the level of the microvasculature of the inner choroid (26 μm below the Bruch membrane) and 1 at the level of large choroidal vessels (the intermediate level between the Bruch membrane and the deepest site of the chorioscleral interface through the fovea). It is reported that choriocapillaris is located about 5–10 μm below the Bruch membrane, and its diameter is about 15–20 μm.[26–28] Each en face image was created by extracting from 3-dimensional raster scans at every 2.6 μm depth. Thus, we decided to measure the choroidal microvascular area 26 μm below the Bruch membrane. The area of choroidal vasculature of the adopted images was measured using ImageJ public domain software (Wayne Rasband, National Institutes of Health, Bethesda, Maryland, USA; available at http://rsb.info.nih.gov/ij/index.html). In ImageJ, the command path Image > Adjust > Threshold > Auto was used to distinguish the

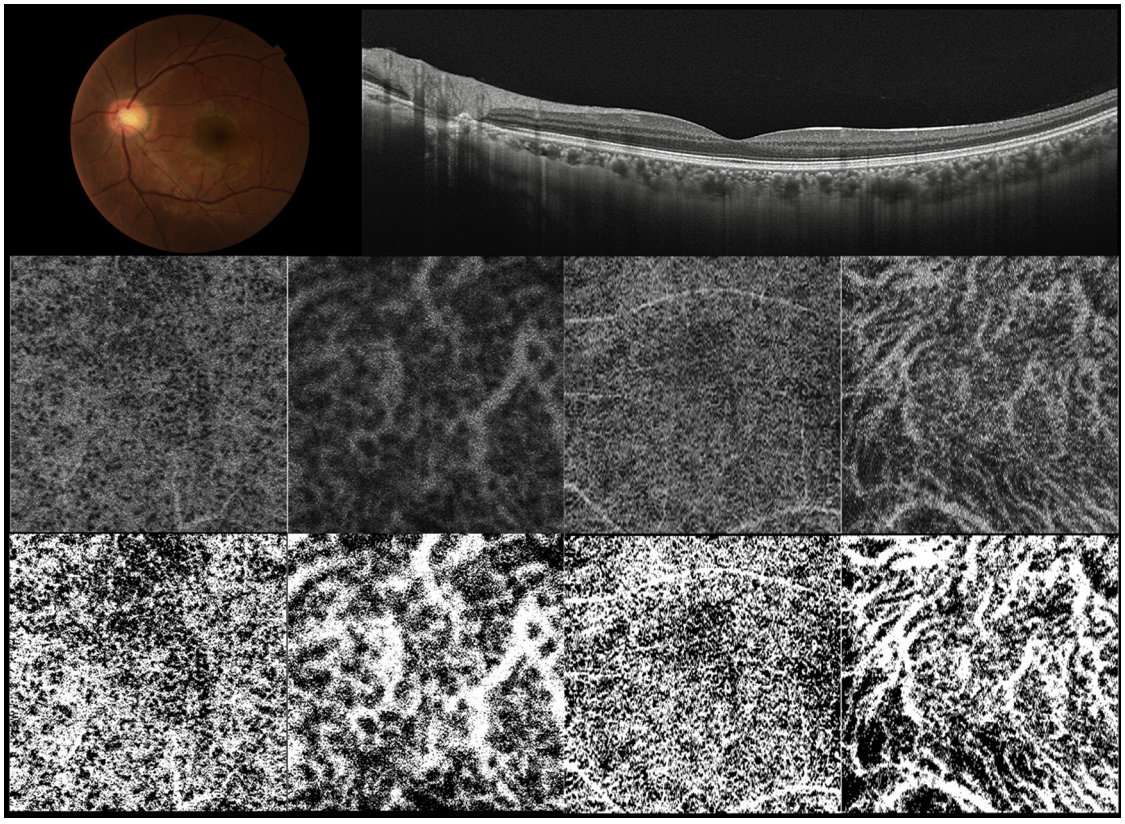

FIGURE 1. Representative images of normal left eye of a 37-year-old man. (Top left) Fundus photograph. (Top right) Horizontal section by swept-source optical coherence tomography. The subfoveal choroidal thickness was 274 μm. (Middle) En face images of choroidal vasculature. (Bottom) Binarized images. The white areas indicate the choroidal vascular area. (Middle left) En face images of 3 × 3 mm at the level of the microvasculature of the inner choroid. (Middle second) En face images of 3 × 3 mm at the level of the large choroidal vessels. (Middle third) En face images of 6 × 6 mm at the level of the microvasculature of the inner choroid. (Middle right) En face images of 6 × 6 mm at the level of the large choroidal vessels. (Bottom left) En face binarized images of 3 × 3 mm at the level of the microvasculature of the inner choroid. (Bottom second) En face binarized images of 3 × 3 mm at the level of the large choroidal vessels. (Bottom third) En face binarized images of 6 × 6 mm at the level of the microvasculature of the inner choroid. (Bottom right) En face binarized images of 6 × 6 mm at the level of the large choroidal vessels.

vasculature and the choroidal stroma, and the adopted images were binarized (Figure 1, Bottom row). Binarization of an en face image was done by the Otsu method, which is an automatic threshold selection method from gray-level histograms.[29] Next, the area of the portion of vascular lumens was calculated in the pixel value by using the command path Analyze > Measure in ImageJ. In the present study, the choroidal vascular area of the adopted images was defined as the percentage of the portion of vascular lumen area against whole scan area.

• **STATISTICAL ANALYSIS:** All values are presented as mean ± standard deviation. The measured visual acuity was converted to the logarithm of the minimum angle of resolution (logMAR) for statistical analyses. χ^2 Tests were used to compare the distribution of categorical variables. Unpaired *t* tests were used to compare with control eyes or between states of CSC. Paired *t* test was used to compare between affected eyes and unaffected fellow eyes in patients with unilateral CSC. One-way analysis of variance (ANOVA) and post hoc Bonferroni test were used to compare among the 3 subtypes of CSC. Bivariate relationships were examined using Pearson product-moment correlation coefficient test. Statistical significance was set at $P < .05$.

RESULTS

IN THIS STUDY, 40 EYES OF 34 PATIENTS WITH CSC AND 26 eyes of 26 healthy subjects were included. Twenty-eight patients had unilateral CSC and 6 patients had bilateral CSC.

• **CENTRAL SEROUS CHORIORETINOPATHY EYES AND UNAFFECTED FELLOW EYES COMPARED WITH CONTROL EYES:** CSC patients and healthy subjects were similar in age (55.4 ± 12.1 vs 56.5 ± 20.5, $P = .797$) and axial length (23.6 ± 1.2 mm vs 24.2 ± 1.2 mm, $P = .060$). There was no significant difference in sex distribution between the CSC

TABLE 1. Choroidal Vascular Areas of Central Serous Chorioretinopathy Eyes and the Unaffected Fellow Eyes Compared With Normal Control Eyes

	Control Eyes (n = 26)	CSC Eyes (n = 40)	Fellow Eyes (n = 28)	*P* Value[a]	*P* Value[b]
Age (y)	56.5 ± 20.5	55.4 ± 12.1	54.07 ± 13.0	.797	.608
Sex (M/F)	12/14	26/14	18/10	.130	.180
R/L	12/14	22/18	16/12	.482	.419
Axial length (mm)	24.2 ± 1.2	23.6 ± 1.2	24.1 ± 1.4	.060	.690
Subfoveal choroidal thickness (μm)	238.0 ± 81.1	395.9 ± 103.3	339.8 ± 101.9	<.001	<.001
Vascular area (%)					
Microvasculature (3 × 3 mm)	52.2 ± 1.8	53.4 ± 2.4	52.9 ± 1.9	.028	.162
Large choroidal vessels (3 × 3 mm)	54.9 ± 4.4	66.9 ± 7.1	62.1 ± 7.1	<.001	<.001
Microvasculature (6 × 6 mm)	51.9 ± 2.1	54.0 ± 1.7	53.4 ± 1.7	<.001	.006
Large choroidal vessels (6 × 6 mm)	53.8 ± 4.3	64.8 ± 7.3	61.0 ± 7.1	<.001	<.001

CSC = central serous choroiretinopathy.
[a]*P* value was compared between the eyes with CSC and normal control eyes.
[b]*P* value was compared between the unaffected fellow eyes in patients with unilateral CSC and normal control eyes.

patients and healthy subjects (26 men and 14 women vs 12 men and 14 women, $P = .130$).

The mean subfoveal choroidal thickness of eyes with CSC (395.9 ± 103.3 μm) was significantly larger compared with control eyes (238.0 ± 81.1 μm). The choroidal vascular area was significantly higher in eyes with CSC than in control eyes both at the level of the microvasculature of the inner choroid (3 × 3 mm: 53.4% ± 2.4% vs 52.2% ± 1.8%, $P = .028$; 6 × 6 mm: 54.0% ± 1.7% vs 51.9% ± 2.1%, $P < .001$) and at the level of the large choroidal vessels (3 × 3 mm: 66.9% ± 7.1% vs 54.9% ± 4.4%, $P < .001$; 6 × 6 mm: 64.8% ± 7.3% vs 53.8% ± 4.3%, $P < .001$) (Table 1, Figures 1 and 2).

Unaffected fellow eyes and control eyes were similar in age ($P = .608$) and axial length ($P = .690$). The mean subfoveal choroidal thickness was larger in the unaffected fellow eyes (339.8 ± 101.9 μm) compared with the control eyes ($P < .001$). The choroidal vascular area was significantly higher in unaffected fellow eyes with CSC than in control eyes at the level of the microvasculature of the inner choroid (6 × 6 mm: 53.4% ± 1.7%, $P = .006$), not at the level of the microvasculature of the inner choroid (3 × 3 mm: 52.9% ± 1.9%, $P = .162$). The choroidal vascular area in the unaffected fellow eyes was larger at the level of the large choroidal vessels (3 × 3 mm: 62.1% ± 7.1%, $P < .001$; 6 × 6 mm: 61.0% ± 7.1%, $P < .001$) than in the control eyes (Table 1).

• **AFFECTED EYES COMPARED WITH UNAFFECTED FELLOW EYES:** Comparisons of parametric data of affected eyes and unaffected fellow eyes of the unilateral CSC patients are shown in Table 2. The mean subfoveal choroidal thickness in the affected eyes was significantly thicker than in the unaffected fellow eyes (384.8 ± 113.8 μm vs 339.8 ± 101.9 μm, $P = .005$). There was no significant difference in the choroidal vascular area at the level of the microvasculature of the inner choroid. The choroidal vascular area at the large choroidal vessels level was significantly larger in the affected eyes than in the unaffected fellow eyes (3 × 3 mm: 65.5% ± 7.1% vs 62.1% ± 7.1%, $P = .012$; 6 × 6 mm: 63.2% ± 7.6% vs 61.0% ± 7.1%, $P = .030$).

• **ACTIVE EYES COMPARED WITH RESOLVED EYES:** Thirty-three eyes were active status with SRD involving the macula and 7 were resolved eyes with absence of SRD. Table 3 shows comparative data between active eyes and resolved eyes. There was no significant difference in the subfoveal choroidal thickness and the choroidal vascular area between active eyes and resolved eyes.

• **COMPARISON AMONG SUBTYPES OF CENTRAL SEROUS CHORIORETINOPATHY:** Of total 40 CSC eyes, 21 were classic CSC, 13 were DRPE, and 6 were MPPE. One-way ANOVA showed significant differences in the axial length and the vascular area at the level of the microvasculature of the inner choroid among the 3 subtypes of CSC (Table 4). In the MPPE type, the vascular area at the level of the microvasculature of the inner choroid (55.8% ± 2.2%) was significantly larger than in the classic type (53.1% ± 2.1%, $P = .038$) and DRPE (52.9% ± 2.6%, $P = .042$). One-way ANOVA indicated no significant difference in the subfoveal choroidal thickness and the vascular area at the level of large choroidal vessels.

• **RELATIONSHIP BETWEEN SUBFOVEAL CHOROIDAL THICKNESS AND CHOROIDAL VASCULAR AREA:** In 40 affected eyes with CSC, there was no statistically significant correlation between the subfoveal choroidal thickness and the choroidal vascular area at the level of the microvasculature of the inner choroid (Figure 3, Top). However, the choroidal vascular area at the level of the large choroidal

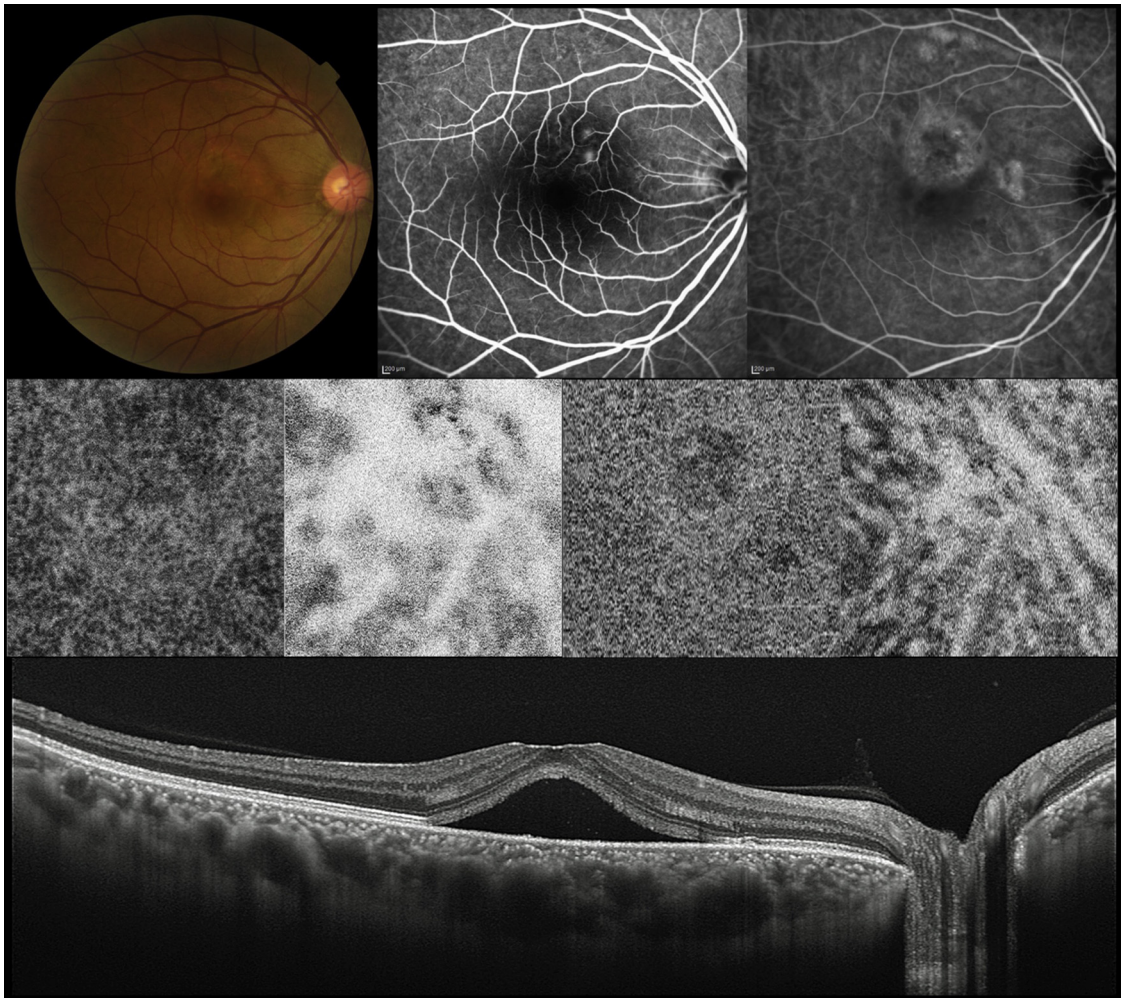

FIGURE 2. Representative images of right eye of a 46-year-old man with active classic central serous chorioretinopathy. (Top left) Fundus photograph shows serous retinal detachment. (Top second) Fluorescein angiography shows a few spots of leakage from the retinal pigment epithelium. (Top right) Indocyanine green angiography shows choroidal hyperpermeability. (Middle) En face images of choroidal vasculature. The white areas indicate the choroidal vascular area. (Middle left) En face image of 3 × 3 mm at the level of the microvasculature of the inner choroid. (Middle second) En face image of 3 × 3 mm at the level of the large choroidal vessels shows extreme choroidal dilation. (Middle third) En face images of 6 × 6 mm at the level of the microvasculature of the inner choroid. (Middle right) En face image of 6 × 6 mm at the level of the large choroidal vessels shows choroidal dilation. (Bottom) The horizontal image through the fovea by swept-source optical coherence tomography shows serous retinal detachment and increased choroidal thickness (532 μm).

vessels was positively correlated with the subfoveal choroidal thickness (Figure 3, Bottom).

DISCUSSION

THE ETIOLOGY OF CSC HAS NOT YET BEEN DETERMINED. However, previous studies using IA showed choroidal vascular abnormalities of eyes with CSC, including delayed filling, vascular congestion, choroidal vascular hyperpermeability, and punctate hyperfluorescent spots,[8–14] suggesting that the primary pathogenesis of CSC is choroidal vascular disturbance.[30] A previous study reported that the abnormalities of RPE and choroid caused serous retinal detachment.[31] The present study evaluated choroidal vasculature of CSC using en face SS-OCT imaging. The results of our study demonstrated that vascular areas of the choroid were larger in eyes with CSC than in age-matched normal controls, which was seen in both diseased eyes and unaffected fellow eyes, both at the level of the microvasculature of the inner choroid and at the large choroidal vessel level.

IA has been the standard approach for examining choroidal vasculature. However, evaluation of choroidal vasculature depends on 2-dimensional assessment with

TABLE 2. Choroidal Vascular Areas of Affected Eyes Compared With Unaffected Fellow Eyes in Central Serous Chorioretinopathy

	Affected Eyes	Fellow Eyes	*P* Value
Axial length (mm)	23.8 ± 1.2	24.1 ± 1.4	.009
Subfoveal choroidal thickness (μm)	384.8 ± 113.8	339.8 ± 101.9	.005
Vascular area (%)			
Microvasculature (3 × 3 mm)	52.8 ± 2.0	52.9 ± 1.9	.890
Large choroidal vessels (3 × 3 mm)	65.5 ± 7.1	62.1 ± 7.1	.012
Microvasculature (6 × 6 mm)	53.7 ± 1.6	53.4 ± 1.7	.398
Large choroidal vessels (6 × 6 mm)	63.2 ± 7.6	61.0 ± 7.1	.030

TABLE 3. Choroidal Vascular Areas of Active Eyes Compared With Resolved Eyes in Central Serous Chorioretinopathy

	Active (n = 33)	Resolved (n = 7)	*P* Value
Age (y)	55.6 ± 11.2	54.3 ± 16.6	.801
Axial length (mm)	23.8 ± 1.1	23.2 ± 1.2	.259
Subfoveal choroidal thickness (μm)	384.8 ± 113.8	438.9 ± 101.9	.229
Vascular area (%)			
Microvasculature (3 × 3 mm)	53.6 ± 2.5	52.6 ± 2.0	.293
Large choroidal vessels (3 × 3 mm)	67.0 ± 7.3	66.5 ± 6.8	.871
Microvasculature (6 × 6 mm)	54.0 ± 1.7	53.6 ± 1.8	.583
Large choroidal vessels (6 × 6 mm)	64.7 ± 7.4	65.7 ± 7.1	.748

overlapping of all choroidal layers. Another limitation is the difficulty in obtaining objective and quantitative measurements. With the advent of OCT, cross-sectional imaging of the choroid has improved its assessment. Using the EDI-OCT technique, several researchers reported that patients with CSC had thick choroid.[16,17] However, most studies using EDI-OCT measured representative points of the choroid, such as subfoveal choroidal thickness. In addition, en face imaging of the choroid is difficult using EDI-OCT. For all the cited reasons, there has been limited information for the 3D profile of the choroid in CSC eyes. Using high-penetrating SS-OCT, we previously reported that increased choroidal thickness is observed in the whole macular area of eyes with any of the CSC subtypes.[20] In the current study, using en face SS-OCT imaging, we quantitatively evaluated choroidal vasculature structures at the microvasculature of the inner choroid and large choroidal vessel levels separately in the macular area.

The choroid is a highly vascular tissue under the sensory retina. The choroidal vasculature is composed of 3 layers: the choriocapillaris adjacent to the Bruch membrane, the Sattler layer with medium-sized vessels, and the Haller layer with large-sized vessels. The choriocapillaris comprises continuous anastomotic vascular networks,[32] which play a key role in nourishing and oxygenating the photoreceptors. The main cause of subretinal fluid accumulation in CSC has been thought to be hyperpermeability in the choriocapillaris, which is demonstrated by the staining of the inner choroid seen on mid-phase IA.[2] The increased permeability in the choriocapillaris is believed to be attributable to stasis, ischemia, or inflammation, but this has not been confirmed.[33] In this study, the choroidal vascular area at the microvasculature of the inner choroid level was larger in eyes with CSC than in age-matched normal eyes, suggesting that choroidal capillaries are dilated in CSC eyes. This finding shows morphologic vascular change of the microvasculature of the inner choroid, implying increased hydrostatic pressure at the choriocapillaris level.

Choroidal thickness in CSC eyes was much greater than that in normal eyes, which is consistent with previous reports.[16,17,20] The current study revealed that choroidal vascular areas at the large choroidal vessel level were larger in eyes with CSC than in age-matched normal eyes. In addition, choroidal vascular area was positively correlated with the choroidal thickness. Choroidal thickening in CSC eyes has been thought to be attributable to choroidal vascular hyperpermeability and increased hydrostatic pressure within the choroid.[16] Our results suggest that thickening of the choroid reflects, at least in part, the morphologic change of choroidal vessels. The extension of choroidal vasculature may result from increase of inflow into the choroidal artery or outflow obstruction through the choroidal vein. The hydrostatic pressure in the choriocapillaris may be increased as well, which would lead to fluid leakage into the subretinal space through the disrupted RPE.

In the unaffected fellow eyes, the vascular area was greater than in age-matched normal eyes. Moreover, the unaffected eyes had larger choroidal thickness than healthy eyes, which is consistent with previous reports.[34] These results indicate that patients with CSC have abnormal choroidal vasculature in both eyes even if only the unilateral eye has symptom of CSC. Meanwhile, the fellow eyes in patients with unilateral CSC have been reported to have RPE changes.[35] Recently, pachychoroid pigment epitheliopathy (PPE) was proposed as a newly clinical entity, which is characterized by RPE abnormalities overlying the areas of choroidal thickening without subretinal fluid.[36] PPE is likely a "forme fruste" of CSC. Later, Pang and Freund have reported that PPE might lead to choroidal neovascularization.[37] Thus, ophthalmologists should carefully observe unaffected fellow eyes in CSC patients, as

TABLE 4. Comparison of Choroidal Vascular Areas Among Subtypes of Central Serous Chorioretinopathy

	Classic (n = 21)	DRPE (n = 13)	MPPE (n = 6)	*P* Value
Age (y)	52.2 ± 12.0	58.2 ± 13.4	60.0 ± 5.9	.224
Axial length (mm)	24.2 ± 1.2	22.9 ± 0.7	23.4 ± 0.9	.005
Subfoveal choroidal thickness (μm)	382.4 ± 113.4	424.8 ± 107.2	380.8 ± 30.4	.412
Vascular area (%)				
Microvasculature (3 × 3 mm)	53.1 ± 2.1	52.9 ± 2.6	55.8 ± 2.2	.029
Large choroidal vessels (3 × 3 mm)	65.6 ± 8.3	68.2 ± 6.0	68.3 ± 4.6	.521
Microvasculature (6 × 6 mm)	53.7 ± 1.8	54.4 ± 1.4	54.1 ± 2.4	.494
Large choroidal vessels (6 × 6 mm)	63.2 ± 7.9	66.7 ± 7.1	66.6 ± 4.4	.335

DRPE = diffuse retinal pigment epitheliopathy; MPPE = multifocal posterior pigment epitheliopathy.

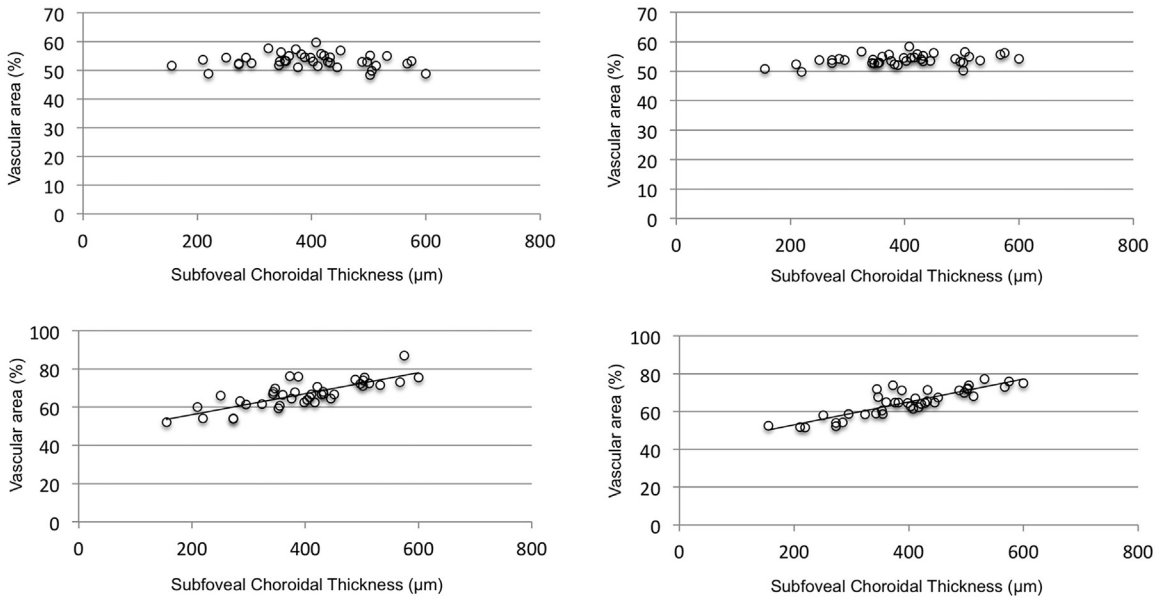

FIGURE 3. Relationship between the subfoveal choroidal thickness and the choroidal vascular area. (Top) The vascular area at the microvasculature of the inner choroid level had no statistically significant correlation with the subfoveal choroidal thickness (left: 3 × 3 mm, $P = .558$; right: 6 × 6 mm, $P = .310$). (Bottom) The choroidal vascular areas at the level of large choroidal vessels were directly proportional to the subfoveal choroidal thickness (left: 3 × 3 mm, $r = .795$, $P < .001$; right: 6 × 6 mm, $r = .861$, $P < .001$).

they, too, are at risk of developing CSC, PPE, or choroidal neovascularization.

There was no difference in choroidal vasculature and choroidal thickness between active and resolved eyes, suggesting that choroidal vasculature remains increased in patients with CSC after resolution of SRD. Further, angiographic choroidal vascular abnormalities persist after resolution of SRD.[13] These findings suggest that choroidal structural change in CSC may exist regardless of leakage from the RPE. These findings may have a relationship with the well-known phenomenon that SRD tends to recur, especially in areas with choroidal hyperpermeability, in patients with CSC. PDT leads to choroidal thinning[17] and encourages long-term choroidal vascular remodeling,[38] whereas focal photocoagulation does not change choroidal thickness.[17] Thus, PDT may have a potential to prevent recurrence of SRD in CSC patients.[39,40]

We classified CSC into 3 subtypes. Some patients with CSC have shown recent onset of the disease with only few specific points of leakage from the RPE; these eyes are termed "classic CSC."[2] Other patients with chronic disease have broad areas of granular hyperfluorescence during FA associated with many indistinct areas of leakage; these are termed "diffuse retinal pigment epitheliopathy (DRPE)."[2] Multifocal posterior pigment epitheliopathy (MPPE) is a severe form of CSC manifesting more extensive SRD, and the hyperpermeability of the choriocapillaris may be the primary pathology in MPPE.[25] Our results

showed that MPPE has the greater vascular area at the level of the microvasculature of the inner choroid than classic and DRPE in the central macular area, suggesting that the hydrostatic pressure of the inner choroid is higher in MPPE eyes. These findings are consistent with the characteristic that MPPE has more severe SRD and poorer visual prognosis than other CSC subtypes. It is also possible that age may be associated with disease severity, though there were no significant differences in age among the subtypes. Spaide and associates reported that older patients were more likely to have DRPE and lower visual acuity.[2] Old age and longer symptom duration are related to more severe RPE damage; thus, the clinical manifestations may vary with age.

The current study had several limitations. First, the sample size was relatively small, especially in resolved CSC eyes and MPPE eyes. Second, the discrimination between choroidal stroma and vasculature by binarization may be rough, and the image binarizing method should be improved to distinguish choroidal stroma and vasculature more clearly. Third, the distance between each B-scan might be inadequate to analyze the fine vasculature of the inner choroid, especially for assessment with 3D 6×6 mm^2 volumetric scans. Moreover, a 6×6 mm en face image inevitably contains a projection of the arcade vessels at the level of the microvasculature of the inner choroid. Therefore, 3×3 mm en face images at the inner choroid level may be more appropriate for analysis by this method. Fourth, it took several minutes to analyze the images in a single case, unless there was an error in the segmentation of the Bruch membrane. If manual corrections were required, it took more than 15 minutes. However, in cases with CSC, the segmentation error was likely to occur only in the location of pigment epithelial detachment. If the segmentation algorithm is improved, this analysis of choroidal vasculature will be more practical. The strengths of this study were prospective inclusion of patients and objective evaluation of the choroidal vasculature by en face SS-OCT images instead of cross-sectional SD OCT images.

In conclusion, we investigated choroidal vasculature in CSC. The results demonstrated that choroidal vascular area was increased in the whole macula area in eyes with CSC. This finding suggests that the underlying physiopathology of CSC might be circulatory disturbance in the choroid. This technique will be informative for observing the changes of the choroidal vessels before and after treatment.

FUNDING/SUPPORT: THIS STUDY WAS SUPPORTED, IN PART, BY THE JAPAN SOCIETY FOR THE PROMOTION OF SCIENCE (JSPS), Tokyo, Japan (Grant-in-Aid for Scientific Research, no. 21592256); the Japan National Society for the Prevention of Blindness, Tokyo, Japan; and the Innovative Techno-Hub for Integrated Medical Bio-Imaging of the Project for Developing Innovation Systems, from the Ministry of Education, Culture, Sports, Science and Technology (MEXT) in Japan. Financial disclosures: Nagahisa Yoshimura: Topcon Corporation, Tokyo, Japan (financial support), Nidek, Gamagori, Japan (financial support, consultant), Canon, Tokyo, Japan (financial support). The following authors have no financial disclosures: Yoshimasa Kuroda, Sotaro Ooto, Kenji Yamashiro, Akio Oishi, Hideo Nakanishi, Hiroshi Tamura, and Naoko Ueda-Arakawa. All authors attest that they meet the current ICMJE criteria for authorship.

REFERENCES

1. Gass JD. Pathogenesis of disciform detachment of the neuroepithelium. *Am J Ophthalmol* 1967;63(3). Suppl:1–139.
2. Spaide RF, Campeas L, Haas A, et al. Central serous chorioretinopathy in younger and older adults. *Ophthalmology* 1996;103(12):2070–2079. discussion 2079–2080.
3. Wang M, Munch IC, Hasler PW, Prunte C, Larsen M. Central serous chorioretinopathy. *Acta Ophthalmol* 2008;86(2):126–145.
4. Iida T, Hagimura N, Sato T, Kishi S. Evaluation of central serous chorioretinopathy with optical coherence tomography. *Am J Ophthalmol* 2000;129(1):16–20.
5. Nicholson B, Noble J, Forooghian F, Meyerle C. Central serous chorioretinopathy: update on pathophysiology and treatment. *Surv Ophthalmol* 2013;58(2):103–126.
6. Robertson DM. Argon laser photocoagulation treatment in central serous chorioretinopathy. *Ophthalmology* 1986;93(7):972–974.
7. Fujimoto H, Gomi F, Wakabayashi T, Sawa M, Tsujikawa M, Tano Y. Morphologic changes in acute central serous chorioretinopathy evaluated by fourier-domain optical coherence tomography. *Ophthalmology* 2008;115(9):1494–1500. 1500.e1491–1500.e1492.
8. Hayashi K, Hasegawa Y, Tokoro T. Indocyanine green angiography of central serous chorioretinopathy. *Int Ophthalmol* 1986;9(1):37–41.
9. Guyer DR, Yannuzzi LA, Slakter JS, Sorenson JA, Ho A, Orlock D. Digital indocyanine green videoangiography of central serous chorioretinopathy. *Arch Ophthalmol* 1994;112(8):1057–1062.
10. Prunte C. Indocyanine green angiographic findings in central serous chorioretinopathy. *Int Ophthalmol* 1995;19(2):77–82.
11. Prunte C, Flammer J. Choroidal capillary and venous congestion in central serous chorioretinopathy. *Am J Ophthalmol* 1996;121(1):26–34.
12. Giovannini A, Scassellati-Sforzolini B, D'Altobrando E, Mariotti C, Rutili T, Tittarelli R. Choroidal findings in the course of idiopathic serous pigment epithelium detachment detected by indocyanine green videoangiography. *Retina* 1997;17(4):286–293.
13. Iida T, Kishi S, Hagimura N, Shimizu K. Persistent and bilateral choroidal vascular abnormalities in central serous chorioretinopathy. *Retina* 1999;19(6):508–512.
14. Tsujikawa A, Ojima Y, Yamashiro K, et al. Punctate hyperfluorescent spots associated with central serous chorioretinopathy as seen on indocyanine green angiography. *Retina* 2010;30(5):801–809.

15. Margolis R, Spaide RF. A pilot study of enhanced depth imaging optical coherence tomography of the choroid in normal eyes. *Am J Ophthalmol* 2009;147(5):811–815.
16. Imamura Y, Fujiwara T, Margolis R, Spaide RF. Enhanced depth imaging optical coherence tomography of the choroid in central serous chorioretinopathy. *Retina* 2009;29(10):1469–1473.
17. Maruko I, Iida T, Sugano Y, Ojima A, Ogasawara M, Spaide RF. Subfoveal choroidal thickness after treatment of central serous chorioretinopathy. *Ophthalmology* 2010;117(9):1792–1799.
18. Esmaeelpour M, Povazay B, Hermann B, et al. Three-dimensional 1060-nm OCT: choroidal thickness maps in normal subjects and improved posterior segment visualization in cataract patients. *Invest Ophthalmol Vis Sci* 2010;51(10):5260–5266.
19. Ikuno Y, Kawaguchi K, Nouchi T, Yasuno Y. Choroidal thickness in healthy Japanese subjects. *Invest Ophthalmol Vis Sci* 2010;51(4):2173–2176.
20. Jirarattanasopa P, Ooto S, Tsujikawa A, et al. Assessment of macular choroidal thickness by optical coherence tomography and angiographic changes in central serous chorioretinopathy. *Ophthalmology* 2012;119(8):1666–1678.
21. Ueda-Arakawa N, Ooto S, Ellabban AA, et al. Macular choroidal thickness and volume of eyes with reticular pseudodrusen using swept-source optical coherence tomography. *Am J Ophthalmol* 2014;157(5):994–1004.
22. Choi W, Mohler KJ, Potsaid B, et al. Choriocapillaris and choroidal microvasculature imaging with ultrahigh speed OCT angiography. *PLoS One* 2013;8(12):e81499.
23. Motaghiannezam R, Schwartz DM, Fraser SE. In vivo human choroidal vascular pattern visualization using high-speed swept-source optical coherence tomography at 1060 nm. *Invest Ophthalmol Vis Sci* 2012;53(4):2337–2348.
24. Ferrara D, Mohler KJ, Waheed N, et al. En face enhanced-depth swept-source optical coherence tomography features of chronic central serous chorioretinopathy. *Ophthalmology* 2014;121(3):719–726.
25. Uyama M, Matsunaga H, Matsubara T, Fukushima I, Takahashi K, Nishimura T. Indocyanine green angiography and pathophysiology of multifocal posterior pigment epitheliopathy. *Retina* 1999;19(1):12–21.
26. Ramrattan RS, van der Schaft TL, Mooy CM, de Bruijn WC, Mulder PG, de Jong PT. Morphometric analysis of Bruch's membrane, the choriocapillaris, and the choroid in aging. *Invest Ophthalmol Vis Sci* 1994;35(6):2857–2864.
27. McLeod DS, Grebe R, Bhutto I, Merges C, Baba T, Lutty GA. Relationship between RPE and choriocapillaris in age-related macular degeneration. *Invest Ophthalmol Vis Sci* 2009;50(10):4982–4991.
28. Olver JM. Functional anatomy of the choroidal circulation: methyl methacrylate casting of human choroid. *Eye (Lond)* 1990;4(Pt 2):262–272.
29. Otsu N. A threshold selection method from gray-level histograms. *IEEE Trans Syst Man Cybern* 1979;9(285-296):62–66.
30. Donald J, Gass M. Pathogenesis of disciform detachment of the neuroepithelium: II. Idiopathic central serous choroidopathy. *Am J Ophthalmol* 1967;63(3):587–615.
31. Yao XY, Marmor MF. Induction of serous retinal detachment in rabbit eyes by pigment epithelial and choriocapillary injury. *Arch Ophthalmol* 1992;110(4):541–546.
32. Yoneya S, Tso MO. Angioarchitecture of the human choroid. *Arch Ophthalmol* 1987;105(5):681–687.
33. Yannuzzi LA. Central serous chorioretinopathy: a personal perspective. *Am J Ophthalmol* 2010;149(3):361–363.
34. Maruko I, Iida T, Sugano Y, Ojima A, Sekiryu T. Subfoveal choroidal thickness in fellow eyes of patients with central serous chorioretinopathy. *Retina* 2011;31(8):1603–1608.
35. Gupta P, Gupta V, Dogra MR, Singh R, Gupta A. Morphological changes in the retinal pigment epithelium on spectral-domain OCT in the unaffected eyes with idiopathic central serous chorioretinopathy. *Int Ophthalmol* 2010;30(2):175–181.
36. Warrow DJ, Hoang QV, Freund KB. Pachychoroid pigment epitheliopathy. *Retina* 2013;33(8):1659–1672.
37. Pang CE, Freund KB. Pachychoroid neovasculopathy. *Retina* 2015;35(1):1–9.
38. Schmidt-Erfurth U, Laqua H, Schlotzer-Schrehard U, Viestenz A, Naumann GO. Histopathological changes following photodynamic therapy in human eyes. *Arch Ophthalmol* 2002;120(6):835–844.
39. Chan WM, Lai TY, Lai RY, Tang EW, Liu DT, Lam DS. Safety enhanced photodynamic therapy for chronic central serous chorioretinopathy: one-year results of a prospective study. *Retina* 2008;28(1):85–93.
40. Chan WM, Lai TY, Lai RY, Liu DT, Lam DS. Half-dose verteporfin photodynamic therapy for acute central serous chorioretinopathy: one-year results of a randomized controlled trial. *Ophthalmology* 2008;115(10):1756–1765.